Enterovirus 71-Induced Autophagy Detected In Vitro and In Vivo Promotes Viral Replication

Shu-Chen Huang, Chia-Lun Chang, Po-Shun Wang, Yu Tsai, and Hsiao-Sheng Liu*

Department of Microbiology and Immunology, College of Medicine, National Cheng Kung University, Tainan, Taiwan

Enterovirus 71 (EV71) is an important pathogen causing death in children under 5 years old worldwide. However, the underlying pathogenesis remains unclear. This study reveals that EV71 infection in rhabdomyosarcoma (RD) and neuroblastoma (SK-N-SH) cells stimulated the autophagic process, which was demonstrated by an increase of punctate GFP-microtubule-associated protein 1 light chain 3 (GFP-LC3), the level of autophagosome-bound LC3-II protein and double-membrane autophagosome formation. EV71-induced autophagy benefited EV71 replication, which was confirmed by the autophagic inducer rapamycin and the inhibitor 3-methyladenine. Signaling pathway investigation revealed that the decreased expression of phosphorylated mTOR and phosphorylated p70S6K is involved in EV71-induced autophagy in a cell-specific manner. The expression of phosphorylated extracellular signal-regulated kinase (Erk) was suppressed consistently in EV71-infected cells. However it did not participate in the autophagic response of the cell. Other signaling pathway molecules, such as Erk, PI3K/Akt, Bcl-2, BNIP3, and Beclin-1 were not affected by infection with EV71. Electron microscopy showed co-localization of autophagosome-like vesicles with either EV71-VP1 or LC3 protein in neurons of the cervical spinal cord in ICR mice infected with EV71. In conclusion, EV71 infection triggered autophagic flux and induced autophagosome formation both in vitro and in vivo. Autophagy induced by EV71 is beneficial for viral replication. Understanding the role of autophagy induced by EV71 in vitro and the formation of autophagosome-like vesicle in vivo provide new insights into the pathogenesis of EV71 infection. *J. Med. Virol. 81:1241–1252, 2009.* © 2009 Wiley-Liss, Inc.

KEY WORDS: EV71; autophagy; autophagosome

INTRODUCTION

EV71 belongs to the human enterovirus A species of the *Enterovirus* genus within the family *Picornaviridae*.

Clinical features of EV71 infection occur most frequently as hand-foot-and-mouth disease. Children under 5 years of age are particularly susceptible to the most severe forms of EV71-associated neurological diseases, including aseptic meningitis, brainstem and/or cerebellar encephalitis, and acute flaccid paralysis [Chang et al., 1999]. In the 1998 outbreak, death was caused by pulmonary edema or pulmonary hemorrhage [Liu et al., 2000; Wang et al., 2000; Yan et al., 2000]. Virus was isolated from different central nervous system (CNS) regions, including medulla oblongata, pons, and spinal cord [Hsueh et al., 2000; Yan et al., 2000]. Histological evidence also showed that neurons degenerate extensively in EV71 infection. The tissue damage in EV71 encephalitis is likely to be caused by virus neurotropism [Hsueh et al., 2000]. Several studies have demonstrated that apoptosis contributes to the death of infected target cells, such as human neurons and endothelial cells in vitro [Kuo et al., 2002; Li et al., 2002; Liang et al., 2004], and the CNS is infected by EV71 in mice and cynomolgus monkeys [Chen et al., 2004; Nagata et al., 2004; Wang et al., 2004]. However, autophagy and its role in EV71-related pathogenesis in EV71-infected cells have not been reported.

Autophagy is a cellular process necessary for the lysosomal degradation and recycling of long-lived proteins and entire organelles. Pathogen infection and other environmental stresses can induce autophagy. Autophagy begins with the isolation of double-membrane structures in the cytoplasm. Later, these membrane structures elongate and mature, and LC3 is recruited to the membrane (LC3 aggregation). The elongated double-membranes form autophagosomes, which sequester cytoplasmic proteins and damaged

organelles such as mitochondria. The autophagosomes become mature with acidification and fuse with lysosomes to become autolysosomes. Eventually, the sequestered contents are degraded by lysosomal hydrolases for recycling, and some studies suggest that these recycled materials help cells to overcome stresses [Abeliovich et al., 2000]. The process of autophagy is tightly regulated by two ubiquitylation-like conjugation systems: Atg12-conjugation and Atg8-lipidation (LC3-modification in mammals) [Wang and Klionsky, 2003].

The reports of autophagy induced by viral infection are accumulating. In cells infected with poliovirus (PV), an accumulation of membrane structures in the cytoplasm during infection has been observed. These structures are composed of double-membranes and contain markers of the rough endoplasmic reticulum, Golgi apparatus and lysosomes [Schlegel et al., 1996]. More recently, LC3 and lysosomal-associated membrane protein 1 (LAMP-1) have been detected in PV- and rhinovirus-induced vesicles in infected cells. In addition, the co-expression of two PV-encoded proteins 2BC and 3A triggers co-localization of LC3 and LAMP-1. Moreover, inhibition of the autophagic process using siRNA to directly knock-down the autophagic proteins LC3 and Atg12 decreases both intracellular and extracellular virus yield. This indicates that viral infection induces the formation of autophagosome-like structures to serve as membrane scaffolds for viral RNA replication and to inhibit the maturation of these structures into degradative organelles [Jackson et al., 2005; Sir et al., 2008]. Autophagy is induced by various viruses such as dengue virus [Lee et al., 2008], coxsackievirus B3 [Wong et al., 2008], rhinovirus types 2 and 14 [Jackson et al., 2005], hepatitis C virus [Ait-Goughoulte et al., 2008; Sir et al., 2008], murine hepatitis virus [Prentice et al., 2004], herpes simplex virus type I [Talloczy et al., 2002], human parvovirus B19 [Nakashima et al., 2006], human immunodeficiency virus type I [Espert et al., 2006], and influenza A virus [Zhou et al., 2009]. In contrast, Brabec-Zaruba et al. [2007] reported that rhinovirus type 2 did not induce autophagosome formation and autophagosomes did not induce viral replication. Therefore, whether autophagy is a general process in response to viral infection remains undetermined. Furthermore, the mechanisms underlying autophagy in virus infection, as well as how the viruses manipulate the autophagic process, remain uncertain.

Autophagosomes are large vesicles with diameters of 400–900 nm in yeast and 500–1,500 nm in mammalian cells. Both yeast Atg8 and its human homologue LC3 proteins are retained in autophagosomal membranes until the maturation is completed. LC3 is a general marker for autophagic membranes. The localization of LC3 in the cell is determined easily by generating the green fluorescent protein GFP-LC3 [Kabeya et al., 2000]. When an autophagosome starts to form, homogeneous cytosolic GFP-LC3 adheres to autophagosomal membranes to form aggregated dots (GFP-LC3 puncta). The LC3 cleaved by Atg4 is called LC3-I, which resides in the cytosol. After ubiquitylation-like modification by

Atg7, LC3 is conjugated to phosphatidylethanolamine (PE), called LC3-II, which associates tightly with the autophagosomal membrane. Usually, two LC3 bands are detected by Western blotting: the smaller LC3-II (16 kDa) and the larger LC3-I (18 kDa). The amount of LC3-II and the LC3-II/LC3-I ratio correlates positively with the number of autophagosomes, and are used widely for quantitation of autophagic processes or autophagosome formation [Kabeya et al., 2000].

The target of rapamycin (TOR) is involved in the autophagic process TOR is an atypical serine/threonine kinase, originally identified genetically in the unicellular budding yeast *Saccharomyces cerevisiae*. Inhibition of TOR kinase by rapamycin induces autophagy in yeast [Noda and Ohsumi, 1998] and malignant glioma cells [Iwamaru et al., 2007]. Reduced TOR activity is also required for the maturation of pre-autophagosomal vesicles into autophagic vacuoles by increasing the expression of autophagy-specific genes such as *ATG8* [Abeliovich et al., 2000]. The homologue of TOR protein in mammalian cells is mTOR. Two similar TOR complexes in yeast have also been identified in mammalian cells. TOR complex 1 in mammalian cells (mTORC1) phosphorylates the two well-characterized mTOR effectors p70 S6 kinase (p70S6K) and eukaryotic initiation factor 4E binding protein 1 (4E-BP1), thereby promoting translation as well as suppressing autophagy under favorable conditions [Wullschleger et al., 2006]. Stimulating the growth receptors that recruit class I phosphatidylinositol 3 kinase (PI3K) or expressing a constitutive active form of protein kinase B (PKB/Akt) inhibits autophagy [Petiot et al., 2000]. Rapamycin reverses most of the inhibition of autophagy mediated by the class I PI3K pathway. The activation of class I PI3K/Akt also relieves the inhibitory effects of the tuberous sclerosis complex (TSC1/TSC2, hamartin/tuberin) on mTOR/p70S6 kinase signaling. In summary, class I PI3K/Akt as well as the downstream target mTOR regulate negatively the autophagic machinery [Cao et al., 2006].

Therefore, experiments were designed to determine whether EV71-infection of the cells induces the formation of autophagosomes both in vitro and in vivo as well as to understand the signaling pathway(s) involved.

MATERIALS AND METHODS

Cell and Virus Culture

Human rhabdomyosarcoma (RD; ATCC, CCL-136) and neuroblastoma (SK-N-SH; ATCC, HTB-11) cells were maintained in L-glutamine containing Dulbecco's modified Eagle's medium (DMEM) (Gibco-BRL, Gaithersburg, MD) supplemented with 10% fetal bovine serum (FBS) (Trace, Sydney, Australia) plus penicillin-streptomycin (200 U/ml), and cultured at 37°C in a 5% CO_2 incubator. At 80% confluence, cells were trypsinized with 0.25% trypsin (Sigma, St. Louis, MO) and sub-cultured in the complete medium. The stock of EV71 (Tainan/4643/98 strain) was propagated for one generation in RD cells before use. The virus titer was

evaluated in RD cells by plaque assay. Mouse-adapted EV71 (MP4 strain) was obtained from Dr. Chun-Keung Yu [Wang et al., 2004]. MP4 EV71 derived from the fourth passage of the parental EV71 was intraperitoneally (i.p.) inoculated into 1-day-old Imprinting Control Region (ICR) mice (Laboratory Animal Center, National Cheng Kung University Medical College, Taiwan), and the virus was isolated from the brain tissues of infected animals by one passage in RD cells. Heat inactivation of EV71 at $65°C$ for 2 hr was used to suppress completely the activity of live viruses.

Virus Plaque Assay

RD cells (5×10^5 cells/well) were plated onto a 12-well plate (TPP, Trasadingen, Switzerland) and incubated overnight. When complete medium was removed, the cells were infected with 10-fold serially diluted virus suspension (200 µl/well). Suspensions were serially diluted in 2% FBS containing DMEM. After absorption at $37°C$ in a 5% CO_2 incubator for 1 hr, the virus suspension was replaced with twofold DMEM containing 0.8% FBS and 1% methyl cellulose (American Biorganics, Niagara Falls, NY). The medium was removed at 72 hr after infection. The cells were washed with phosphate-buffered saline (PBS), and then fixed and stained with 5% crystal violet at $37°C$ for 1 hr. Finally, the crystal violet was washed out with water and heat-dried at $37°C$. The titer of the virus was represented as plaque forming units (pfus) per milliliter.

Transfection

RD or SK-N-SH cells (4×10^5 cells/well) were seeded onto six-well plates (TPP) and incubated overnight. The cells were transfected with 5 µg of pEGFPC1-LC3 plasmid DNA [Kabeya et al., 2000] using the lipofection method (Lipofectin® reagent, Invitrogen, Carlsbad). After incubation at $37°C$ in 5% CO_2 for the appropriate time, the cells were analyzed as indicated for each experiment.

In Vitro Virus Infection

For in vitro virus infection experiments, 2×10^6 or 3×10^6 cells were seeded onto 10 cm cell culture dishes (TPP) and incubated overnight. After the medium was replaced with 2% FBS containing DMEM, cells were infected with EV71 (4643 strain), heat-inactivated virus or mock-treated (the same growth medium but without virus) at $37°C$ in a 5% CO_2 incubator for 1 hr. The cells were then cultured in fresh complete DMEM for various times as indicated. For autophagy induction experiments, the cells were pre-treated with tamoxifen (10 µM; Sigma) and rapamycin (100 nM; Sigma) for 2 hr, infected with EV71 or mock-treated for 1 hr, and then cultured in fresh complete DMEM containing tamoxifen or rapamycin for the indicated times. For autophagy inhibition experiments, cells were infected with EV71 in medium with 3-methyladenine (3-MA) (10, 20, or 30 mM) (Sigma) for different times as indicated.

Cell Lysate Collection and Western Blotting

At the indicated times after EV71 infection, culture medium was removed and cells were re-suspended in 150 µl of modified RIPA lysis buffer (1 mM Na_3VO_4, 2 mM EGTA, 0.5% aprotenin, 1% leupeptin, and 1 mM PMSF) per 10 cm cell culture dish. After lysis at $4°C$, the supernatant was normalized for equal protein content (BCA assay, Pierce, Rockford, IL). Samples (50 µg protein per lane) were separated via sodium dodecyl sulfate–polyacrylamide gel electrophoresis (SDS–PAGE) (8% polyacrylamide for mTOR and p70S6K; 12% polyacrylamide for beclin 1, Bcl-2, BNIP3 and ERK; 15% polyacrylamide for Akt and LC3). Proteins were transferred to the PVDF membrane (Perkin Elmer Life Sciences, Inc., Boston, MA) and the membrane was incubated at RT with 5% non-fat dried milk in TBST for 1 hr. Membranes were incubated overnight at $4°C$ with primary antibodies in TBST. Primary antibodies specific for p-mTOR (ser2448), mTOR, p-p70S6K (thr389), p70S6K, and p-Akt (thr308) were from Cell Signaling (Beverly, MA); p-Erk1/2, Erk1/2, and beclin 1 were from Santa Cruz Biotechnology, Inc. (Santa Cruz, CA); BNIP3 and β-actin were from Sigma; Bcl-2 was from BD (Franklin Lakes, NJ); and LC3 was from Abgent (San Diego, CA). Membranes were washed with TBST and incubated with a 1:5,000 dilution of anti-rabbit (Amersham Pharmacia, Piscataway, NJ) or anti-mouse (Chemicon, Temecula, CA) IgG antibody conjugated with horseradish peroxidase at RT for 1 hr. The immuno-reactive bands detected by ECL reagents (Millipore, Billerica, MA) were developed with Super RX film (Fuji film, Tokyo, Japan) or detected directly with a BioSpectrum Imaging system (UVP, Upland, CA). The Western blotting results were quantified by densitometric analysis using VisionWorks™ LS image acquisition and analysis software (UVP).

Transmission Electron Microscopy

After infection, the cells were fixed with 2.5% glutaraldehyde in 0.1 M cacodylate buffer containing 4% sucrose, 1 mM $MgCl_2$, and 1 mM $CaCl_2$, and post-fixed in 1% osmium tetroxide. The cells were then dehydrated in a gradient series of ethanol and embedded with LR White (Agar Scientific, Stansted, UK). Ultrathin sections were cut on an ultramicrotome (Reichert-Jung, Heidelberg, Germany) and stained with saturated aqueous uranyl acetate and lead citrate at RT, and then observed under a Hitachi 7000 transmission electron microscope (Hitachi, Tokyo, Japan).

Immunofluorescent Staining

Cells cultured in 6-cm culture dishes were transfected with 5 µg of pEGFPC1-LC3 [Kabeya et al., 2000]. The aggregation of GFP-LC3 was detected using an inverted microscope (Leica AM6000, Giessen, Germany).

EV71 was detected using monoclonal anti-EV71 VP1 antibody (MAB979, Chemicon) followed by labeling with rhodamine (TRITC)-conjugated goat anti-mouse IgG

monoclonal antibody (Jackson Immuno Research, West Grove, PA). Non-specific fluorescence was blocked using the secondary antibody. The cells were observed under a confocal scanning microscope (Olympus FB1000, Tokyo, Japan).

Immuno-Staining Electron Microscopy

For mouse infection experiments, the EV71 MP4 strain at 5×10^6 pfu per mouse was orally inoculated into 7-day-old ICR mice after 8 hr of fasting. Nine mice were sacrificed at day 5 after infection. After deep anesthesia with 7% chloral hydrate, all mice were perfused with 4% paraformaldehyde in 0.1 M phosphate buffer (PB). After fixation, the cervical spinal cord was removed and kept in PB solution overnight at 4°C. The cervical cord was cut into 100 μm sections. Floating sections were rinsed several times in 0.1 M PB, and washed with Tris buffer solution (TBS), and then treated in a solution containing 1% hydrogen peroxide in TBS for 30 min to remove endogenous peroxidase activity. After washing in TBS, half of the sections were blocked in a combination of 0.01% Triton X-100 and 10% normal horse serum (for anti-mouse antibody, anti-EV71 VP1), and the other half was blocked in a combination of 0.01% Triton X-100 and 10% normal goat serum (for anti-rabbit antibody, anti-LC3) at RT for 1 hr. The sections were then incubated at RT overnight with monoclonal anti-EV71 VP1 antibody (1:3,000; MAB979; Chemicon) and polyclonal anti-LC3 antibody (1:100; MAP1LC3B; Abgent). After incubation, sections were washed in TBS and treated with the secondary antibody, biotinylated horse anti-mouse IgG or biotinylated goat anti-rabbit IgG (1:200; Vector, Burlingame, CA) at RT for 1 hr. After washing with TBS, the reaction was amplified with streptavidin–biotin-peroxidase complex (1:300; DAKO, Carpinteria, CA) and immuno-stained with the chromogen 3, 3-diaminobenzidine tetrahydrochloride (DAB; Sigma). Brown-stained sections were post-fixed in 1% OsO_4 at RT for 1 hr. After osmication, floating sections were briefly rinsed three times in PB, and then dehydrated in 100% ethanol. All specimens were embedded in an Epon-1, 2-propylene oxide mixture (1:1) overnight. Finally, they were embedded in pure Epon at 65°C.

Statistical Analysis

The percentages of cells with increase in GFP-LC3 puncta and virus titers are expressed as mean ± standard deviation. Differences of virus titer compared to control were analyzed by Student's t test.

RESULTS

EV71 Infection Induces GFP-LC3 Puncta in RD and SK-N-SH Cells

The two target cell lines of EV71, RD (muscle) and SK-N-SH (neuron) were used to assess autophagy induced by EV71 infection. These cells were transfected with green fluorescent LC3 plasmid DNA (pEGFPC1-LC3),

an autophagy marker, for 24 hr followed by EV71 infection. When the GFP-LC3 gene was expressed, a homogeneous distribution of GFP-LC3 was seen in the cells. When autophagy was induced, GFP-LC3 protein aggregated to form puncta in the cells. After RD (Fig. 1A) and SK-N-SH (Fig. 1C) cells were infected with live EV71 for 6 hr, GFP-LC3 puncta formation was seen. The most abundant of puncta formation (>44%) occurred at 9 hr after infection and then it declined at 12 hr (Fig. 1B,D). GFP-LC3 and EV71 VP1 protein were co-localized in the same cells, indicating that cells with abundant GFP-LC3 puncta were indeed affected by EV71 (Fig. 1E). These findings indicate that EV71 infection induces the formation of GFP-LC3 puncta in muscle cells and neurons.

EV71 Infection Increases LC3-II Expression in RD and SK-N-SH Cells

When autophagy occurs, LC3-I protein undergoes a lipidation modification mediated by Atg7 to the smaller LC3-II protein and then binds to the double-membrane autophagosome. Therefore, the level of LC3-II expression was used to represent the degree of autophagy. LC3-II expression was greatly induced in RD and SK-N-SH cells at 9 hr after infection, and the levels are maintained at 12 hr (Fig. 2A,B). The LC3-II level was dramatically decreased after 12 hr because of extensive cell death (data not shown). The expression of EV71 VP1 protein was detected from 6 hr after infection in RD cells (Fig. 2A). Taken together, the present data demonstrated that autophagy was induced in RD and SK-N-SH cells by EV71 infection.

Autophagosome- and Autolysosome-Like Structures, Together With EV71 Particles, Occur in the Cytoplasm of EV71-Infected Cells

To further confirm that autophagy is induced by EV71 infection, SK-N-SH cells with or without EV71 were observed under transmission electron microscopy. Double-membrane vesicles engulfing cytosolic materials were seen in the cytoplasm of infected cells but not in uninfected cells (Fig. 3A,B). EV71 virus aggregates and single-layer autolysosome-like vesicles were also seen (Fig. 3C). The numbers of these single- and double-layer vesicles decreased in infected cells pretreated with 3-MA, an autophagy inhibitor [Seglen and Gordon, 1982] (Fig. 3D), indicating that these vesicles were autophagy-related structures. The data reveal that autophagosome- and autolysosome-like vesicles, together with EV71 particles, occurred in the cytoplasm of cells infected with EV71.

EV71 Infection-Induced Autophagy Enhances Virus Titer

To clarify the influence of autophagy on EV71 replication, we measured extracellular virus production in culture supernatant of infected SK-N-SH and RD cells when autophagy was inhibited by 3-MA. The number of
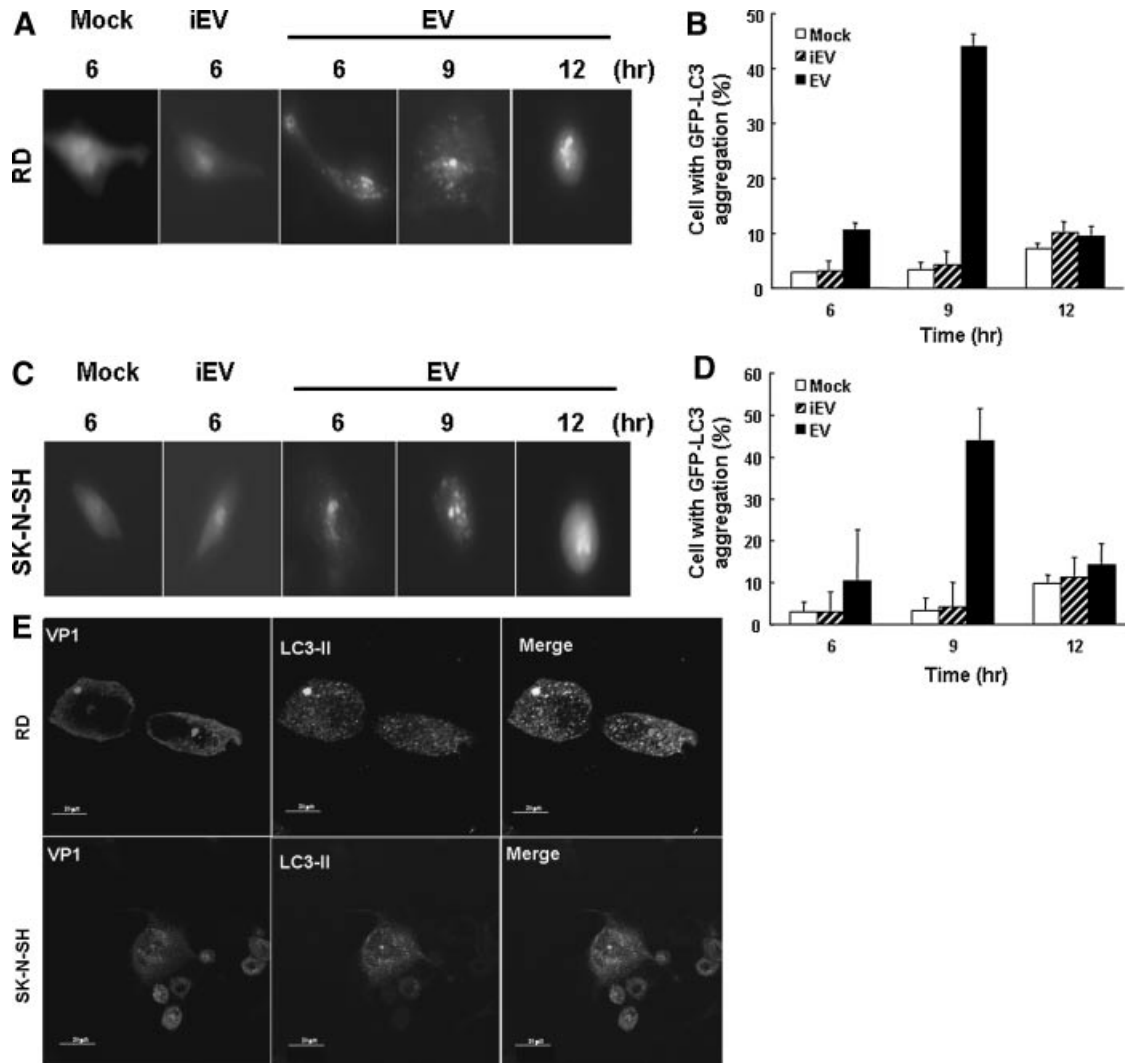
Fig. 1. Formation of GFP-LC3 puncta in EV71 infected RD and SK-N-SH cells. RD (**A**) and SK-N-SH (**C**) cells were transfected with pEGFPC1-LC3 plasmid for16 hr, followed by EV71 (4643 strain) infection for 6, 9, and 12 hr at a MOI of 1 and then observed under the fluorescent microscope. The percentage of the cell with punctated GFP-LC3 was counted in the total GFP expression RD cells (**B**) and SK-N-SH cells (**D**). A total of 100 cells showing green fluorescence were examined for increased GFP-LC3 puncta. **E**: The cells were infected with EV71 for 9 hr. The cells were then treated with anti-EV71 VP1 antibody (MAB979, Chemicon) and anti-LC3 antibody followed by rhodamine (TRITC)-conjugated goat anti-mouse IgG antibody and FITC-conjugated goat anti-rabbit antibody labeling and observed under the confocal microscope. At least 10 fields were examined, and representative images are shown. Mock, uninfected cells; iEV, heat inactivated EV71; EV, live EV71.

GFP-LC3 puncta decreased in the presence of 3-MA in EV71-infected SK-N-SH cells (Supplementary data 1), indicating that 3-MA inhibits EV71-induced autophagy. The extracellular virus titers in the culture supernatant of infected SK-N-SH cells treated with 10, 20, or 30 mM 3-MA during infection were evaluated by plaque assay. The extracellular virus titers decreased as the dose of 3-MA increased at 6, 9, and 12 hr after infection (Fig. 4A). The extracellular virus production in EV71-infected SK-N-SH cells was assessed when autophagy was induced either by serum starvation or by the autophagy inducers, tamoxifen [Bursch et al., 1996], or rapamycin [Noda and Ohsumi, 1998]. SK-N-SH cells were pretreated with tamoxifen (10 μM), rapamycin (100 nM), or incubated in the medium without serum for 2 hr, and then infected with EV71 (MOI = 1). Consistently, extracellular virus titers were markedly increased under the same conditions after 3 hr of infection (Fig. 4B). We also demonstrated that GFP-LC3 puncta increased under serum starvation or after treatment with autophagy inducers in SK-N-SH cells at 3, 6, and 9 hr after infection (Supplementary data 2). Further, the effect of an autophagy inhibitor (3MA) and an inducer (tamoxifen) on autophagic activity (LC3-II) and virus replication (VP1) was demonstrated by Western blotting. Consistently, the Western blotting data showed a positive correlation between the expression levels of LC3 II and EV 71 VP1 proteins (Fig. 4C,D). Rapamycin and tamoxifen showed no side effect on the cells at the concentrations used (Supplementary data 5).
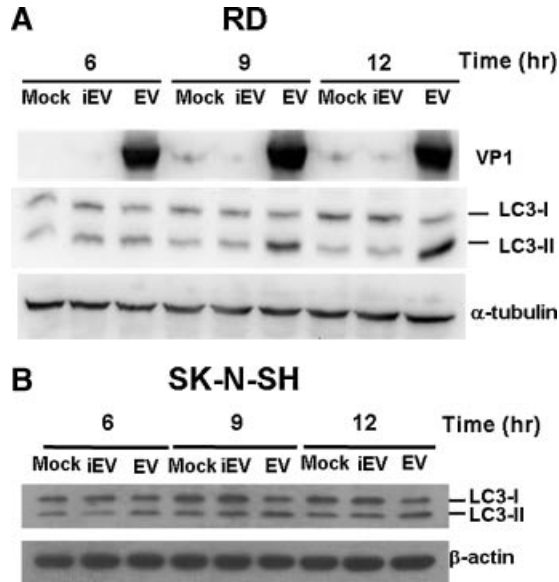
Fig. 2. The expression levels of LC3-I and LC3-II protein in RD and SK-N-SH cells infected with EV71. RD (**A**) and SK-N-SH (**B**) cells were infected by EV71 (4643 strain). The same procedure used in Figure 1 was conducted. The expression of VP1, LC3-I and LC3-II protein was detected using anti-EV71 VP1 antibody (MAB979, Chemicon) and anti-LC3 antibody (Abgent) by Western blot analysis. α-tubulin and β-actin were used as the internal controls. Mock, uninfected cells; iEV, heat inactivated EV71; EV, live EV71; VP, EV71 VP1 protein.

Similar results were seen in infected RD cells (data not shown). In summary, the present data demonstrated that virus replication was promoted by EV71-induced autophagy.
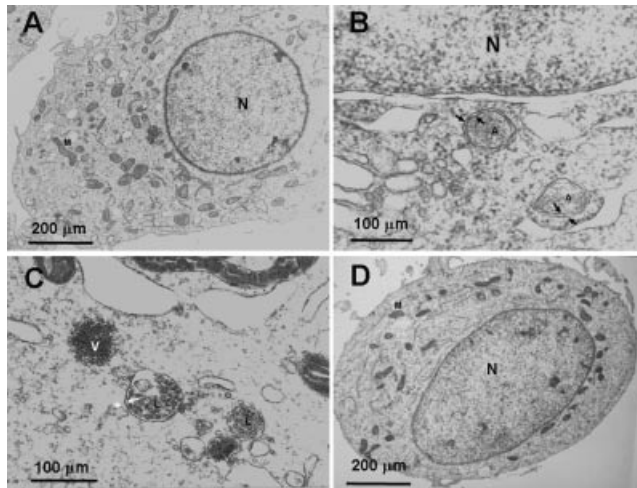

Fig. 3. Detection of EV71 particles and autophagosome-like vesicles in infected SK-N-SH cells by transmission electron microscopy. SK-N-SH cells were infected with EV71 at a MOI of 1 for 6 hr. **A**: Uninfected cells; (**B,C**) cells infected with EV71; (**D**) cells were pretreated 3-MA (100 mM) for 2 hr followed by EV71 infection for 6 hr. Black arrow indicates double-membrane structure; A, autophagosome-like vesicle; white arrow indicates single-membrane structure; L, autolysosome-like vesicle; N, nucleus; M, mitochondria; V, an aggregate of EV71 particles (25–30 nm).

Signaling Pathways Affected by EV71 Infection in RD and SK-N-SH Cells

To determine the signaling pathway affected by EV71 infection, the expression levels of Erk/phosphorylated Erk (p-Erk at tyrosine 204), mTOR/phosphorylated mTOR (p-mTOR at serine 2448), BNIP3, Bcl-2, and Beclin 1 in SK-N-SH cells were monitored by Western blotting. The expression level of p-Erk in SK-N-SH cells was suppressed as early as 15 min after infection and maintained at the same level until 12 hr (Supplementary data 3A and Fig. 5A). The expression level of p-Erk in RD cells also decreased from 6 hr after infection (Fig. 5C). In EV71-infected SK-N-SH cells, the expression level of p-mTOR was unchanged compared with the mock control from 15 to 60 min (Supplementary data 3B). However, the level of p-mTOR evidently decreased from 6 to 12 hr (Fig. 5A). In contrast, in infected RD cells, no suppression of total mTOR and p-mTOR protein was detected (Supplementary data 4 and Fig. 5D). The expression levels of Erk, mTOR, BNIP3, Bcl-2, and Beclin 1 were not affected by infection in both cell lines. These results suggested that EV71 suppression of p-Erk is a general event but the suppression of p-mTOR protein is cell-type specific.

mTOR/p70S6K Signaling Pathway Is Involved in Autophagy Induced by EV71 Infection

Class I PI3K/Akt/mTOR and Erk1/2 signaling pathways are involved in the suppression of autophagy in cancer cells [Arico et al., 2001]. To clarify whether these molecules participate in EV71 infection-induced autophagy, SK-N-SH cells were harvested at 6 hr after infection. The expression levels of LC3, phosphorylated Akt (p-Akt), total mTOR, p-mTOR, total p70S6K, and phosphorylated p70S6K (p-p70S6K) were evaluated by Western blotting. The expression levels of m-TOR, p70S6K, and p-Akt were not altered in infected cells compared to control (Fig. 6, lane 1 vs. 3). The expression levels of p-mTOR and p-p70S6K proteins decreased in infected SK-N-SH cells (Fig. 6A, lane 1 vs. 3), confirming the previous results (Fig. 5A). LC3-II expression increased in infected cells (Fig. 6, lane 1 vs. 3), indicating that autophagy was induced at this time. To confirm further that mTOR and p70S6K signaling are involved in EV71 infection-induced autophagy, the inhibitor of mTOR, rapamycin, was used. The cells were pretreated with rapamycin (100 nM) for 2 hr, and then infected with EV71. In mock control cells, the expression levels of p-mTOR and p-p70S6K decreased in the presence of rapamycin (Fig. 6A, lane 1 vs. 2), showing that rapamycin inhibits effectively p-mTOR. The increased LC3-II expression after rapamycin treatment showed that this drug induced autophagy by inhibiting p-mTOR (Fig. 6A, lane 1 vs. 2). The inhibition of p-mTOR and p-p70S6K became stronger in the presence of rapamycin, accordingly, LC3-II expression was further enhanced during EV71 infection (Fig. 6A, lane 3 vs. 4). Regardless of the presence or absence of rapamycin, the expression levels of p-Akt, total m-TOR, and p70S6K proteins in
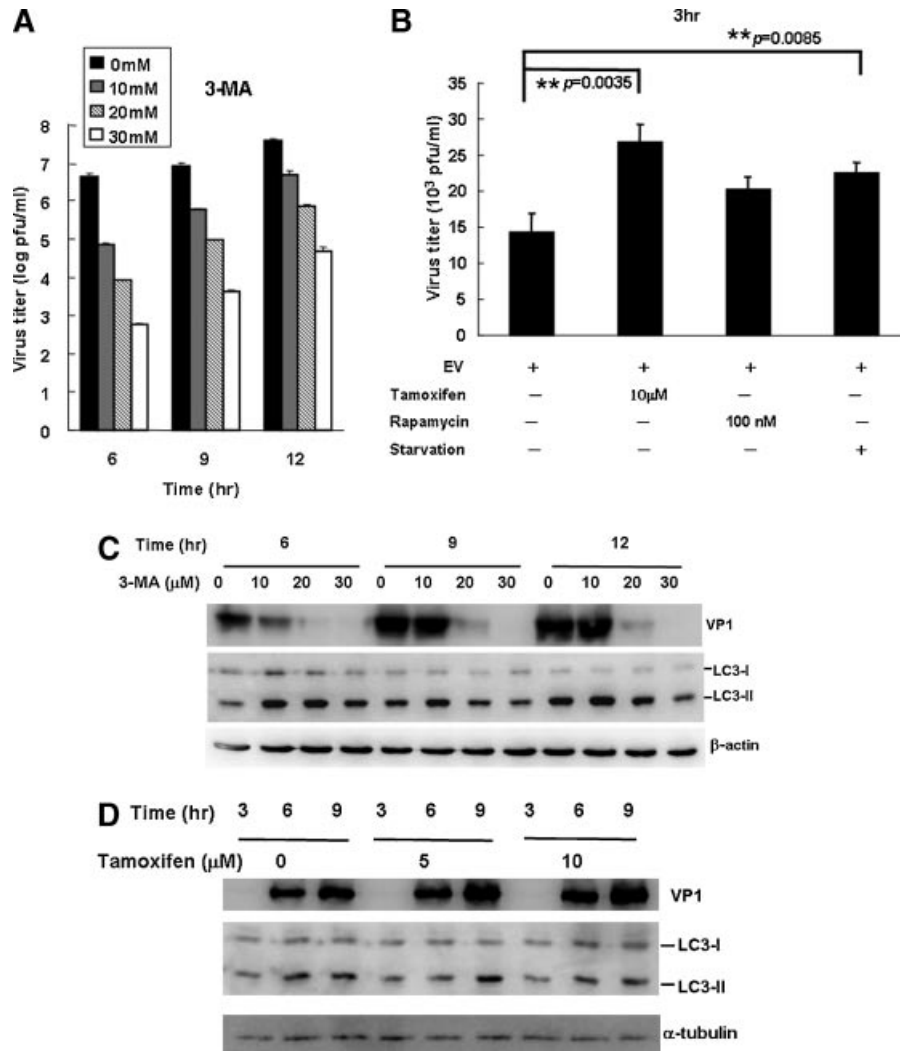
Fig. 4. Effect of various treatments on the titer of EV71 in infected SK-N-SH cells. SK-N-SH cells were infected with EV71 for 6, 9, and 12 hr at the MOI of 1 in medium with 3-MA (10, 20, or 30 mM) (**A**); or pretreated with tamoxifen (10 μM), rapamycin (100 nM) or starvation for 2 hr and then infected by EV71 for 3 hr (**B**). Supernatant was collected and virus titer was determined by plaque assay using RD cells. Data were repeated three times independently and analyzed by Student's *t* test. **P < 0.01. The same treatments used in (A) and (B) were conducted to measure the effect of 3MA (**C**) and tamoxifen (**D**) on the expression of EV71 VP1 and autophagy LC3 proteins by Western blotting.

infected cells did not differ from mock controls (Fig. 6A, lanes 3 and 4 vs. 1 and 2). In addition, rapamycin treatment caused a band shift of p70S6K in both infected and mock-infected cells (Fig. 6A, lanes 2 and 4 vs. 1 and 3). Furthermore, the expression of total PI3K protein was not affected by EV71 infection (data not shown).

To determine the role of Erk1/2 in EV71-induced autophagy, EGF (10 ng/ml) was added to the cells for various time periods to activate Erk by phosphorylation at tyrosine 204 (p-Erk) before harvesting the infected cells. EGF effectively induced Erk1/2 phosphorylation 10 min after treatment (Fig. 6B, lane 4). However, EGF did not reverse the EV71-dependent suppression of Erk phosphorylation (Fig. 6B, lane 6). In contrast, LC3-II expression induced by EV71 was suppressed by EGF treatment (Fig. 6B, lane 3 vs. lane 6), indicating that

Erk1/2 phosphorylation at tyrosine 204 is not needed for EV71-induced autophagy. The effect of EGF on Erk1/2 phosphorylation diminished 30 min after treatment (Fig. 6B, lane 7).

Overall, the above data confirmed that suppression of mTOR and p70S6K phosphorylation contributes to the induction of autophagy in EV71-infected SK-N-SH cells.

Autophagosome-Like Vesicles Appear in Mouse Spinal Neurons After Oral Infection of Mouse-Adapted EV71

Having demonstrated that autophagy is induced in EV71-infected cells in vitro, we then determined whether autophagy can also be induced in vivo. To
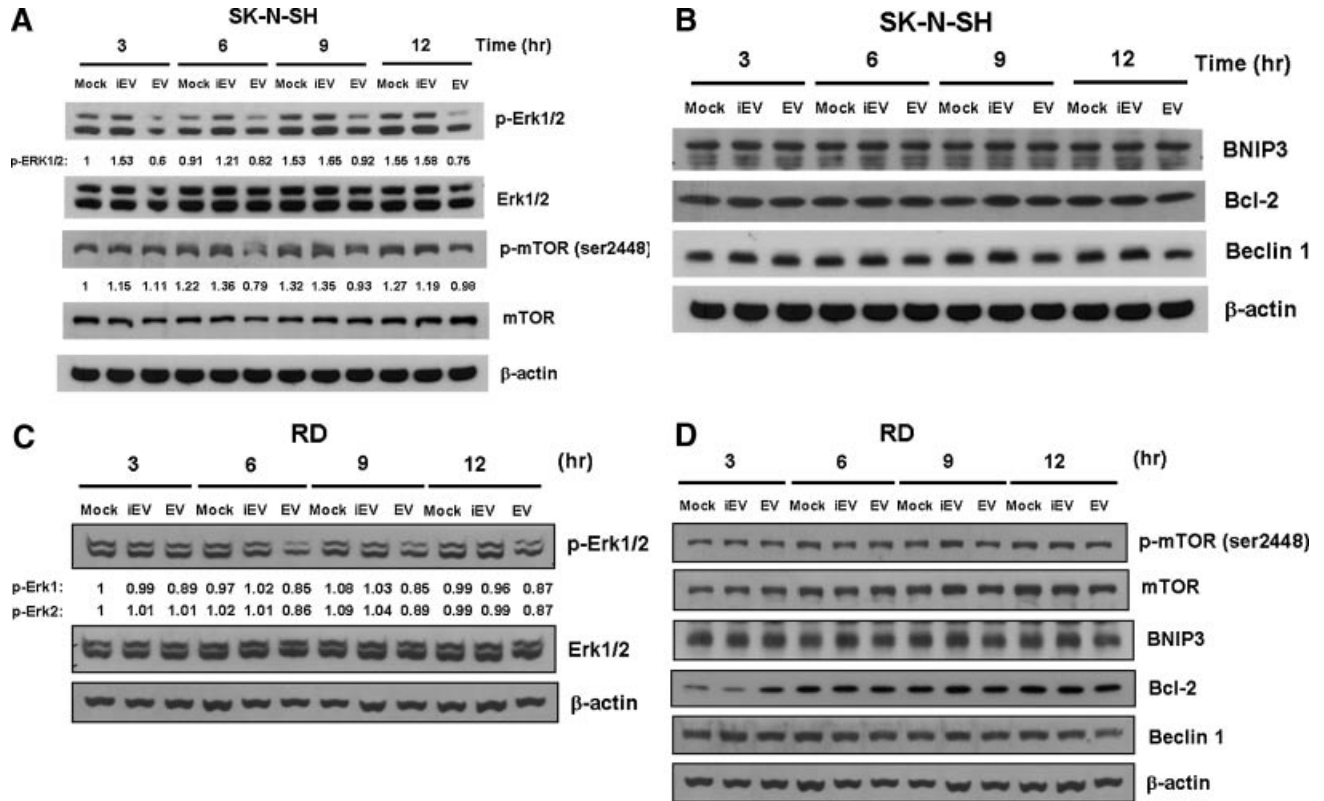
Fig. 5. Signaling pathways involved in EV71 infection of SK-N-SH and RD cells. Cells were infected with EV71 for 3, 6, 9, and 12 hr. Total protein was then harvested and the expression levels of the target proteins were determined using specific antibodies by Western blotting. (**A**) Erk1/2, p-Erk1/2, mTOR, and p-mTOR expression in SK-N-SH cells; (**B**) BNIP3, Bcl-2, and Beclin1 expression in SK-N-SH cells; (**C**) Erk1/2, and p-Erk1/2 expression in RD cells; (**D**) mTOR, p-mTOR, BNIP3, Bcl-2 and Beclin1 expression in RD cells. The band intensity of p-mTOR and p-Erk1/2 was quantified and normalized using the mock control 3 hr after infection as the baseline (set to 1). β-actin was an internal control. Mock, uninfected cells; iEV, heat inactivated EV71; EV, live EV71; p-mTOR, phosphorylated mTOR; p-Erk1/2, phosphorylated Erk1/2.

investigate EV71 infection in mice, a model which mimics the natural route of EV71 infection was utilized. Mice can be infected orally by mouse-adapted EV71 (MP4 strain), which infects CNS neurons [Wang et al., 2004]. Therefore, autophagosome formation in neurons in the cervical spinal cord from EV71-infected mice was investigated. After oral inoculation with EV71, nine mice were sacrificed after 5 days. At this stage, the EV71 titers are maximal (10^2–10^4 pfu/mg) in the cervical spinal cord [Wang et al., 2004]. Neurons from the cervical spinal cord were initially examined by immuno-electron microscopy for the presence and distribution of both EV71 and LC3 protein. To screen for immuno-reactive cells which expressed either EV71 VP1 or LC3 protein, sections were hybridized with the specific antibody. These sections were further investigated for autophagosome formation under TEM. In the EV71 VP-1 antibody-labeled cells (Fig. 7A), autophagosome-like vesicles were detected in the cytoplasm, and the size was 100–500 nm in diameter. Similarly, in LC3-labeled immuno-reactive cells, double-membrane autophagosome-like vesicles were detected in the cytoplasm (Fig. 7B). Autophagosome-like vesicles about 100 nm in diameter were also detected in the cytoplasm of LC3 antibody-labeled immuno-reactive cells, and no inclusions inside the vesicle were detected. Furthermore,

both lipidated LC3 II and EV 71 VP1 proteins were detected by Western blotting in the cervical spinal cord (Fig. 7C). These data indicate that EV71 infection of neurons in the mouse cervical spinal cord induces the formation of autophagosome-like vesicles surrounded by VP1 and LC3 proteins.

DISCUSSION

In this study, it was revealed that GFP-LC3 protein formed puncta (Fig. 1) and LC3-II protein expression was induced in two major EV71 target cell lines: human muscle RD and neuronal SK-N-SH cells (Fig. 2). Double-membrane autophagosome-like structures, single membrane autolysosome-like vesicles and EV71 viral particle aggregates were also detected in EV71-infected SK-N-SH cells (Fig. 3). These results clearly demonstrate that EV71 induces autophagy, and the formation of autophagosome- and autolysosome-like vesicles in vitro. Furthermore, double-membrane autophagosome-like vesicles surrounded by LC3 and EV71 VP1 proteins, as well as EV71 VP1 and LC3 II proteins were detected in neurons from the cervical spinal cord of EV71-infected ICR mice, indicating that EV71 induces autophagy in vivo (Fig. 7).
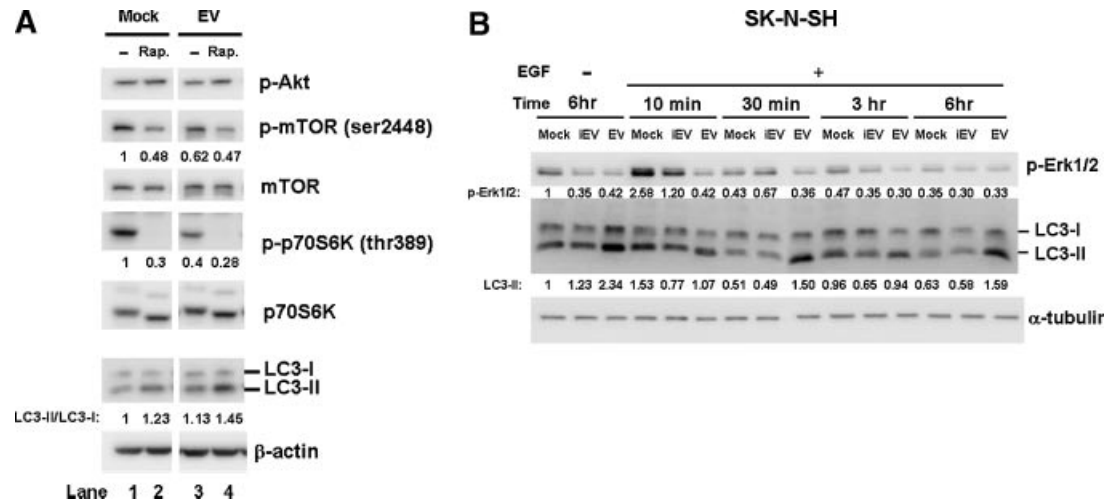
Fig. 6. The involvement of Erk and Akt-mTOR-p70S6K signaling pathways in EV71 induced autophagy in SK-N-SH cells. **A**: SK-N-SH cells were pretreated with rapamycin (100 nM) for 2 hr, and then infected by EV71 for 6 hr at the MOI of 10 in medium with the drug. Total protein was collected from the cells and p-Akt, p-mTOR, mTOR, p-p70S6K, p70S6K, LC3-I, and LC3-II expression was determined by Western blotting. The band intensity was quantified and normalized using the mock control as the baseline (set to 1). **B**: SK-N-SH cells were infected by EV71 and treated with EGF (10 ng/ml) for various time intervals to activate Erk by phosphorylation at tyrosine 204 (p-Erk). All the cells were harvested at 6 hr after infection. The band intensity was quantified and normalized using the mock control as the baseline (set to 1). Either β-actin or α-tubulin was used as the internal control. Mock, untreated cells; EV, active EV71. p-Akt, phosphorylated Akt; p-mTOR, phosphorylated mTOR; p-p70S6K, phosphorylated p70S6K; p-Erk1/2, phosphorylated pErk1/2.

An accumulation of membrane-like structures in the cytoplasm early after infection have been reported with other picornaviruses (poliovirus, coronavirus, coxsackievirus B3, and rhinovirus) [Schlegel et al., 1996; Wong et al., 2008]. Co-localization of viral RNA replication complex with double-membrane vesicles in infected cells has been well documented [Kirkegaard et al., 2004; Wileman, 2006; Espert et al., 2007; Lee et al., 2008; Miller and Krijnse-Locker, 2008; Wong et al., 2008]. Plus stranded RNA viruses induce membrane proliferations that support the replication of their genomes [Miller and Krijnse-Locker, 2008]. Clusters of double-membrane vesicles have also been observed in dengue virus replication complex. Using an anti-double-stranded-RNA (dsRNA) antibody, Panyasrivanit et al. [2009] reveal that amphisomes are formed by the fusion of endosomes and autophagosomes, and these structures are the sites of at least part of the DENV replication/translation complex. Thus, the autophagosome, a double-membrane vesicle, may serve as the site for viral RNA replication. In contrast, infection with rhinovirus does not induce autophagosome formation, and autophagy has no effect on viral replication [Brabec-Zaruba et al., 2007]. Further, ATG5 and the intact autophagic pathway are not required for the replication of murine hepatitis virus [Zhao et al., 2007]. Therefore, whether the autophagosome is a common cellular component utilized by RNA viruses to facilitate their replication remains contradictory. In this study, we demonstrated that autophagy induced by EV71 infection facilitated its own replication. This was further confirmed by using the autophagic inhibitor 3-MA, starvation, or the inducers rapamycin or tamoxifen (Fig. 4). EV71 infection induced the formation of double-membrane autophagosomes, which were surrounded by LC3 and EV71 VP1 proteins

(Fig. 7). Jackson et al. [2005] postulated that viral particles are released from autophagosome-like vesicles, which serve as membrane scaffolds for viral RNA replication. Also, the virus inhibits the maturation of these structures into degradative organelles, due to the co-existence of LC3 and the poliovirus capsid protein VP1 in extracellular structures adjacent to poliovirus-infected cells. Co-localization of LC3 with LAMP1 or with NS1 in dengue virus-infected cells has been reported and postulated that the autophagosome structure may serve as a scaffold docking site for NS1-dsRNA replication complex to promote virus replication inside cells [Mackenzie et al., 1996; Lee et al., 2008; Panyasrivanit et al., 2009]. HCV infection induces the unfolded protein response and the accumulation of autophagosomes in cells without enhancing autophagic protein degradation. This accumulation supports HCV replication (Sir et al., 2008).

The genome of EV71 contains an AU-rich element, and LC3 is a binding protein of an AU-rich RNA element in the 3′-untranslated region of fibronectin mRNA, which facilitates the recruitment of RNA to polyribosomes for translation [Zhou et al., 1997]. Similar to coxsackievirus B3 replication [Wong et al., 2008], it is possible that autophagosome double-membrane vesicles not only act as sites of viral RNA synthesis but also take an active role in viral protein synthesis by bridging the nascent viral RNA with polyribosomes through LC3 in EV71-infected cells. In EV71-infected cells, LC3-II protein was dramatically degraded after 12 hr of infection, which was caused either by progression of autophagic flux or by death of the infected cells.

In SK-N-SH cells, decreased expression levels of p-mTOR and p-p70S6K were associated with the induction of autophagy. However, this relationship
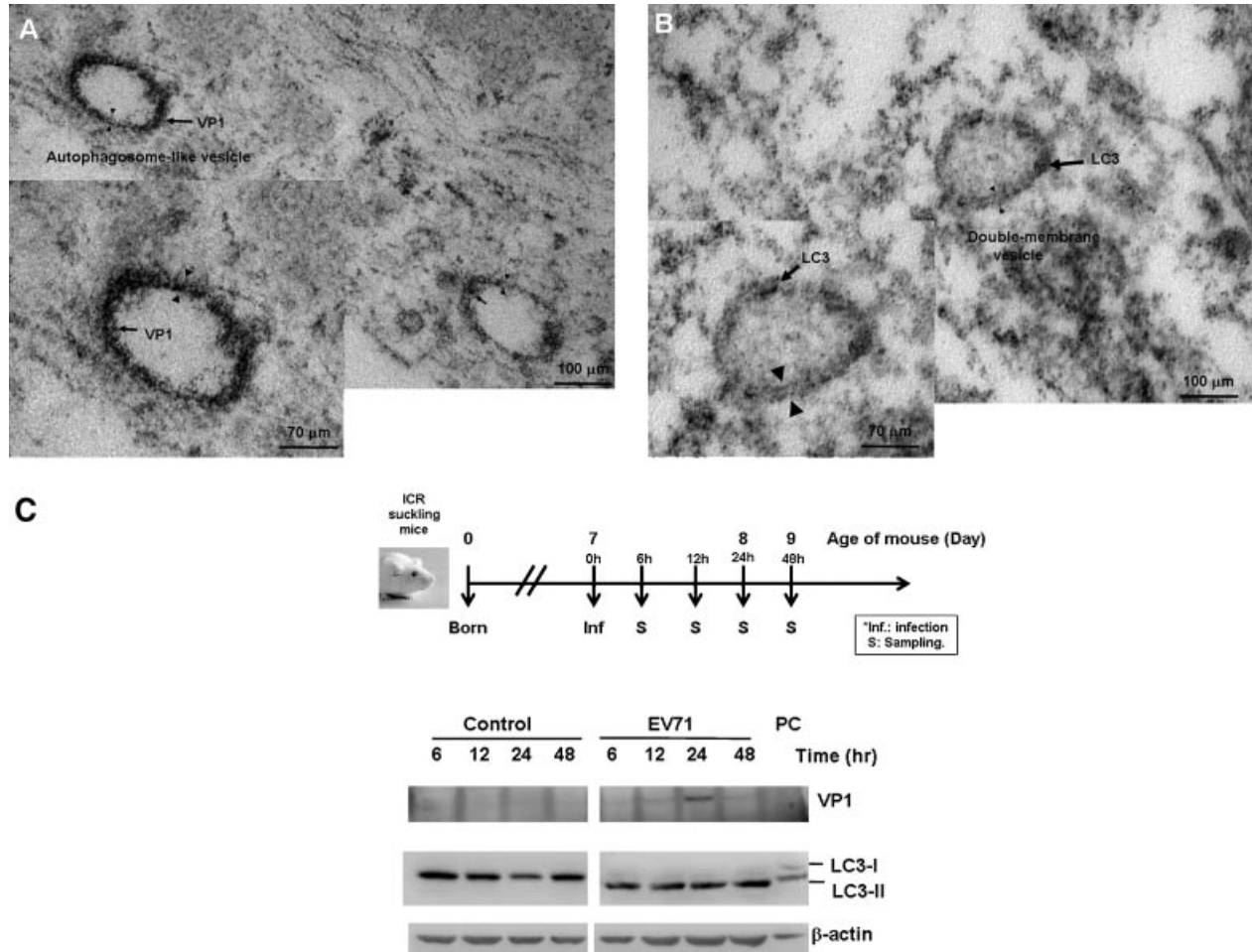
Fig. 7. Detection of autophagosome-like vesicles, LC3 II and VP1 proteins in the neuron cells of mice orally infected by EV71. EV71 (MP4 strain; 5×10^6 pfu) was orally inoculated into 7-day-old ICR mice. Nine mice were sacrificed 5 days after infection. After perfusion and fixation, the cervical spinal cords were collected. Half of vibratome-cut sections were treated with anti-VP1 antibody to detect EV71 (**A**), and the remaining sections were treated with anti-LC3 antibody to detect LC3 distribution (**B**). Antibody responsive sections were immuno-stained with chromogen DAB and counter-stained with uranyl acetate and lead citrate. Positive reaction was detected as dark-stained dots. Sections with brown staining were examined under a JOEL JEM-1400 TEM. In immuno-reactive cells, autophagosome-like vesicles (arrowheads) appeared in the cytoplasm and surrounded by EV71 VP1 (A, arrow). In immuno-reactive cells, double-membrane autophagosome-like vesicles (arrowheads) surrounded by LC3 protein (arrow). **C**: Total protein extracted from cervical spinal cords of EV71 infected and control mice was analyzed for VP1 and LC3 expression using specific antibodies by Western blotting. PC: The protein extracted from cells expressing LC-I and LC-II.

was not seen in infected RD cells, indicating that EV71 may utilize different signaling pathways to induce autophagy in different cells. The levels of total PI3K and the phosphorylation of Akt were not affected by EV71 infection (Fig. 6A). Taken together, it is hypothesized that EV71 infection utilizes mTOR/p70S6K signaling pathway to induce autophagy, and the upstream signal transducer is through a signaling pathway that is independent of class I PI3K/Akt. Further verification of the role of mTOR in EV71-induced autophagy and the effect of mTOR on EV71 replication is needed. Pattingre et al. [2003a,b] reported that upregulation of p-Erk1/2 is involved in autophagy. Activated Erk1/2 directly phosphorylates TSC2 at sites different from the Akt target sites, thereby causing functional inactivation of the TSC1-TSC2 complex and ultimately mTORC1 activation [Ma et al., 2005]. Erk1/2 phosphorylation at tyrosine 204 was suppressed in infected SK-N-SH and

RD cells, but its expression level had no effect on EV71-induced autophagy.

Electron microscopy of cells infected with poliovirus showed that the virus-induced double-membrane vesicles enclose viral particles and/or cytosolic material [Schlegel et al., 1996]. Organelles were not detected inside the autophagosome-like vesicles in infected cells. However, EV71 particles forming aggregates were detected nearby the single-layered autolysome-like vesicles (Fig. 3C). Poliovirus replication proteins 2C and 3D are localized to double-membrane vesicles as demonstrated by immuno-labeling experiments [Schlegel et al., 1996]. Another group demonstrated that these double-membrane vesicles contained poliovirus capsid protein VP1 and LC3 [Jackson et al., 2005]. The present findings of EV71 VP1 and LC3 proteins n double-membrane vesicles support the hypothesis that the autophagosomal membrane serves as a platform for

viral RNA replication complexes and enhances virus replication [Wileman, 2006].

Finally, it was confirmed that specific viral proteins encoded by EV71 contributed to the inhibition of the mTOR/p70S6K pathway and the induction of autophagy. Therefore, different mutants of EV71 proteins and single viral protein expression constructs need to be developed and tested. The formation of autophagosome-like vesicles in the neurons of infected mice indicates that autophagy also occurs in response to EV71 infection in vivo. The above finding suggests that autophagy may play a role in the pathogenesis of EV71 causing neuronal damage, and that autophagy inhibitors, such as 3-MA, may be used for the treatment of EV71 infection.

ACKNOWLEDGMENTS

REFERENCES

Abeliovich H, Dunn WA, Jr., Kim J, Klionsky DJ. 2000. Dissection of autophagosome biogenesis into distinct nucleation and expansion steps. J Cell Biol 151:1025–1034.

Ait-Goughoulte M, Kanda T, Meyer K, Ryerse JS, Ray RB, Ray R. 2008. Hepatitis C virus genotype 1a growth and induction of autophagy. J Virol 82:2241–2249.

Arico S, Petiot A, Bauvy C, Dubbelhuis PF, Meijer AJ, Codogno P, Ogier-Denis E. 2001. The tumor suppressor PTEN positively regulates macroautophagy by inhibiting the phosphatidylinositol 3-kinase/protein kinase B pathway. J Biol Chem 276:35243–35246.

Brabec-Zaruba M, Berka U, Blaas D, Fuchs R. 2007. Induction of autophagy does not affect human rhinovirus type 2 production. J Virol 81:10815–10817.

Bursch W, Ellinger A, Kienzl H, Torok L, Pandey S, Sikorska M, Walker R, Hermann RS. 1996. Active cell death induced by the anti-estrogens tamoxifen and ICI 164 384 in human mammary carcinoma cells (MCF-7) in culture: The role of autophagy. Carcinogenesis 17:1595–1607.

Cao C, Subhawong T, Albert JM, Kim KW, Geng L, Sekhar KR, Gi YJ, Lu B. 2006. Inhibition of mammalian target of rapamycin or apoptotic pathway induces autophagy and radiosensitizes PTEN null prostate cancer cells. Cancer Res 66:10040–10047.

Chang LY, Lin TY, Huang YC, Tsao KC, Shih SR, Kuo ML, Ning HC, Chung PW, Kang CM. 1999. Comparison of enterovirus 71 and coxsackie-virus A16 clinical illnesses during the Taiwan entero-virus epidemic, 1998. Pediatr Infect Dis J 18:1092–1096.

Chen YC, Yu CK, Wang YF, Liu CC, Su IJ, Lei HY. 2004. A murine oral enterovirus 71 infection model with central nervous system involvement. J Gen Virol 85:69–77.

Espert L, Denizot M, Grimaldi M, Robert-Hebmann V, Gay B, Varbanov M, Codogno P, Biard-Piechaczyk M. 2006. Autophagy is involved in T cell death after binding of HIV-1 envelope proteins to CXCR4. J Clin Invest 116:2161–2172.

Espert L, Codogno P, Biard-Piechaczyk M. 2007. Involvement of autophagy in viral infections: Antiviral function and subversion by viruses. J Mol Med 85:811–823.

Hsueh C, Jung SM, Shih SR, Kuo TT, Shieh WJ, Zaki S, Lin TY, Chang LY, Ning HC, Yen DC. 2000. Acute encephalomyelitis during an outbreak of enterovirus type 71 infection in Taiwan: Report of an autopsy case with pathologic, immunofluorescence, and molecular studies. Mod Pathol 13:1200–1205.

Iwamaru A, Kondo Y, Iwado E, Aoki H, Fujiwara K, Yokoyama T, Mills GB, Kondo S. 2007. Silencing mammalian target of rapamycin signaling by small interfering RNA enhances rapamycin-induced autophagy in malignant glioma cells. Oncogene 26:1840–1851.

Jackson WT, Giddings TH, Jr., Taylor MP, Mulinyawe S, Rabinovitch M, Kopito RR, Kirkegaard K. 2005. Subversion of cellular autophagosomal machinery by RNA viruses. PLoS Biol 3:e156.

Kabeya Y, Mizushima N, Ueno T, Yamamoto A, Kirisako T, Noda T, Kominami E, Ohsumi Y, Yoshimori T. 2000. LC3, a mammalian homologue of yeast Apg8p, is localized in autophagosome mem-branes after processing. EMBO J 19:5720–5728.

Kirkegaard K, Taylor MP, Jackson WT. 2004. Cellular autophagy: Surrender, avoidance and subversion by microorganisms. Nature Rev 2:301–314.

Kuo RL, Kung SH, Hsu YY, Liu WT. 2002. Infection with enterovirus 71 or expression of its 2A protease induces apoptotic cell death. J Gen Virol 83:1367–1376.

Lee YR, Lei HY, Liu MT, Wang JR, Chen SH, Jiang-Shieh YF, Lin YS, Yeh TM, Liu CC, Liu HS. 2008. Autophagic machinery activated by dengue virus enhances virus replication. Virology 374:240–248.

Li ML, Hsu TA, Chen TC, Chang SC, Lee JC, Chen CC, Stollar V, Shih SR. 2002. The 3C protease activity of enterovirus 71 induces human neural cell apoptosis. Virology 293:386–395.

Liang CC, Sun MJ, Lei HY, Chen SH, Yu CK, Liu CC, Wang JR, Yeh TM. 2004. Human endothelial cell activation and apoptosis induced by enterovirus 71 infection. J Med Virol 74:597–603.

Liu CC, Tseng HW, Wang SM, Wang JR, Su IJ. 2000. An outbreak of enterovirus 71 infection in Taiwan, 1998: Epidemiologic and clinical manifestations. J Clin Virol 17:23–30.

Ma L, Chen Z, Erdjument-Bromage H, Tempst P, Pandolfi PP. 2005. Phosphorylation and functional inactivation of TSC2 by Erk implications for tuberous sclerosis and cancer pathogenesis. Cell 121:179–193.

Mackenzie JM, Jones MK, Young PR. 1996. Immunolocalization of the dengue virus nonstructural glycoprotein NS1 suggests a role in viral RNA replication. Virology 220:232–240.

Miller S, Krijnse-Locker J. 2008. Modification of intracellular membrane structures for virus replication. Nature Rev 6:363–374.

Nagata N, Iwasaki T, Ami Y, Tano Y, Harashima A, Suzaki Y, Sato Y, Hasegawa H, Sata T, Miyamura T, Shimizu H. 2004. Differential localization of neurons susceptible to enterovirus 71 and poliovirus type 1 in the central nervous system of cynomolgus monkeys after intravenous inoculation. J Gen Virol 85:2981–2989.

Nakashima A, Tanaka N, Tamai K, Kyuuma M, Ishikawa Y, Sato H, Yoshimori T, Saito S, Sugamura K. 2006. Survival of parvovirus B19-infected cells by cellular autophagy. Virology 349:254–263.

Noda T, Ohsumi Y. 1998. Tor, a phosphatidylinositol kinase homologue, controls autophagy in yeast. J Biol Chem 273:3963–3966.

Panyasrivanit M, Khakpoor A, Wikan N, Smith DR. 2009. Co-localization of constituents of the dengue virus translation and replication machinery with amphisomes. J Gen Virol 90:448–456.

Pattingre S, Bauvy C, Codogno P. 2003a. Amino acids interfere with the ERK1/2-dependent control of macroautophagy by controlling the activation of Raf-1 in human colon cancer HT-29 cells. J Biol Chem 278:16667–16674.

Pattingre S, De Vries L, Bauvy C, Chantret I, Cluzeaud F, Ogier-Denis E, Vandewalle A, Codogno P. 2003b. The G-protein regulator AGS3 controls an early event during macroautophagy in human intestinal HT-29 cells. J Biol Chem 278:20995–21002.

Petiot A, Ogier-Denis E, Blommaart EF, Meijer AJ, Codogno P. 2000. Distinct classes of phosphatidylinositol 3'-kinases are involved in signaling pathways that control macroautophagy in HT-29 cells. J Biol Chem 275:992–998.

Prentice E, Jerome WG, Yoshimori T, Mizushima N, Denison MR. 2004. Coronavirus replication complex formation utilizes components of cellular autophagy. J Biol Chem 279:10136–10141.

Schlegel A, Giddings TH, Jr., Ladinsky MS, Kirkegaard K. 1996. Cellular origin and ultrastructure of membranes induced during poliovirus infection. J Virol 70:6576–6588.

Seglen PO, Gordon PB. 1982. 3-Methyladenine: Specific inhibitor of autophagic/lysosomal protein degradation in isolated rat hepatocytes. Proc Natl Acad Sci USA 79:1889–1892.

Sir D, Chen WL, Choi J, Wakita T, Yen TS, Ou JH. 2008. Induction of incomplete autophagic response by hepatitis C virus via the unfolded protein response. Hepatology 48:1054–1061.

Talloczy Z, Jiang W, Virgin HWT, Leib DA, Scheuner D, Kaufman RJ, Eskelinen EL, Levine B. 2002. Regulation of starvation- and virus-

induced autophagy by the eIF2alpha kinase signaling pathway. Proc Natl Acad Sci USA 99:190–195.

Wang CW, Klionsky DJ. 2003. The molecular mechanism of autophagy. Mol Med 9:65–76.

Wang JR, Tsai HP, Chen PF, Lai YJ, Yan JJ, Kiang D, Lin KH, Liu CC, Su IJ. 2000. An outbreak of enterovirus 71 infection in Taiwan, 1998. II. Laboratory diagnosis and genetic analysis. J Clin Virol 17:91–99.

Wang YF, Chou CT, Lei HY, Liu CC, Wang SM, Yan JJ, Su IJ, Wang JR, Yeh TM, Chen SH, Yu CK. 2004. A mouse-adapted enterovirus 71 strain causes neurological disease in mice after oral infection. J Virol 78:7916–7924.

Wileman T. 2006. Aggresomes and autophagy generate sites for virus replication. Science 312:875–878.

Wong J, Zhang J, Si X, Gao G, Mao I, McManus BM, Luo H. 2008. Autophagosome supports coxsackievirus B3 replication in host cells. J Virol 82:9143–9153.

Wullschleger S, Loewith R, Hall MN. 2006. TOR signaling in growth and metabolism. Cell 124:471–484.

Yan JJ, Wang JR, Liu CC, Yang HB, Su IJ. 2000. An outbreak of enterovirus 71 infection in Taiwan 1998: A comprehensive pathological, virological, and molecular study on a case of fulminant encephalitis. J Clin Virol 17:13–22.

Zhao Z, Thackray LB, Miller BC, Lynn TM, Becker MM, Ward E, Mizushima NN, Denison MR, Virgin HWT. 2007. Coronavirus replication does not require the autophagy gene ATG5. Autophagy 3:581–585.

Zhou B, Boudreau N, Coulber C, Hammarback J, Rabinovitch M. 1997. Microtubule-associated protein 1 light chain 3 is a fibronectin mRNA-binding protein linked to mRNA translation in lamb vascular smooth muscle cells. J Clin Invest 100:3070–3082.

Zhou Z, Jiang X, Liu D, Fan Z, Hu X, Yan J, Wang M, Gao GF. 2009. Autophagy is involved in influenza A virus replication. Autophagy 5:1–8.